Supporting Information

Polyacrylamide exotemplate-assisted synthesis of hierarchically porous nanostructured TiO$_2$ macrobeads for efficient photodegradation of organic dyes and microbes

Muhammad Ahmad Mudassir,[†,‡,§] Syed Zajif Hussain,[†] Mishal Khan,[Ŧ] Syeda Tasmia Asma,[†,¶] Zafar Iqbal,[†] Zille Huma,[†] Najeeb Ullah,[¥] Haifei Zhang,[§] Tariq Mahmood Ansari,[*,‡] and Irshad Hussain[*,†,¥]

[†]Department of Chemistry & Chemical Engineering, SBA School of Science & Engineering (SBASSE), Lahore University of Management Sciences (LUMS), Lahore - 54792, Pakistan

[‡]Institute of Chemical Sciences, Bahauddin Zakariya University (BZU), Multan - 60800, Pakistan

[§]Department of Chemistry, University of Liverpool, Oxford Street, Liverpool - L69 3BX, U.K.

[¶]Institute of Industrial Biotechnology (IIB), GC University Lahore - 54000, Pakistan

[Ŧ]Preston Institute of Nano Science & Technology (PINSAT), Islamabad, Pakistan

[¥]US-Pakistan Center for Advanced Studies in Energy (USPCAS-E), University of Engineering & Technology (UET), Peshawar, Pakistan

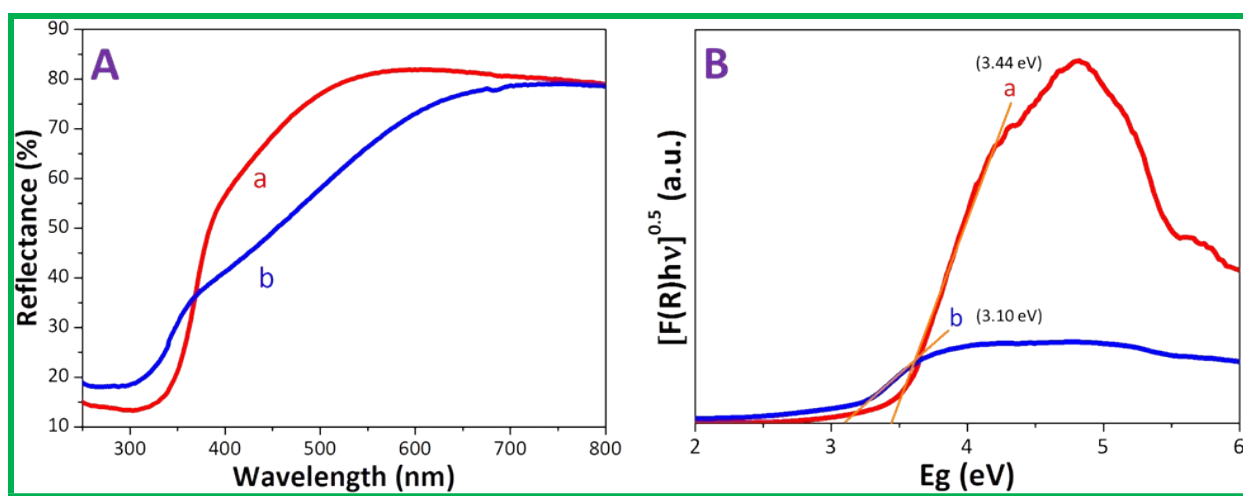*Corresponding authors' email addresses: ihussain@lums.edu.pk; drtariq2000@gmail.com

Figure S1. (A) UV−vis diffuse reflectance spectra and (B) plot of Kubelka-Munk function (F(R)h$v^{0.5}$) versus photon energy (Eg) for the bandgap measurement of (a) PAM−TiO$_2$ NC, and (b) porous NS TiO$_2$ macrobeads.
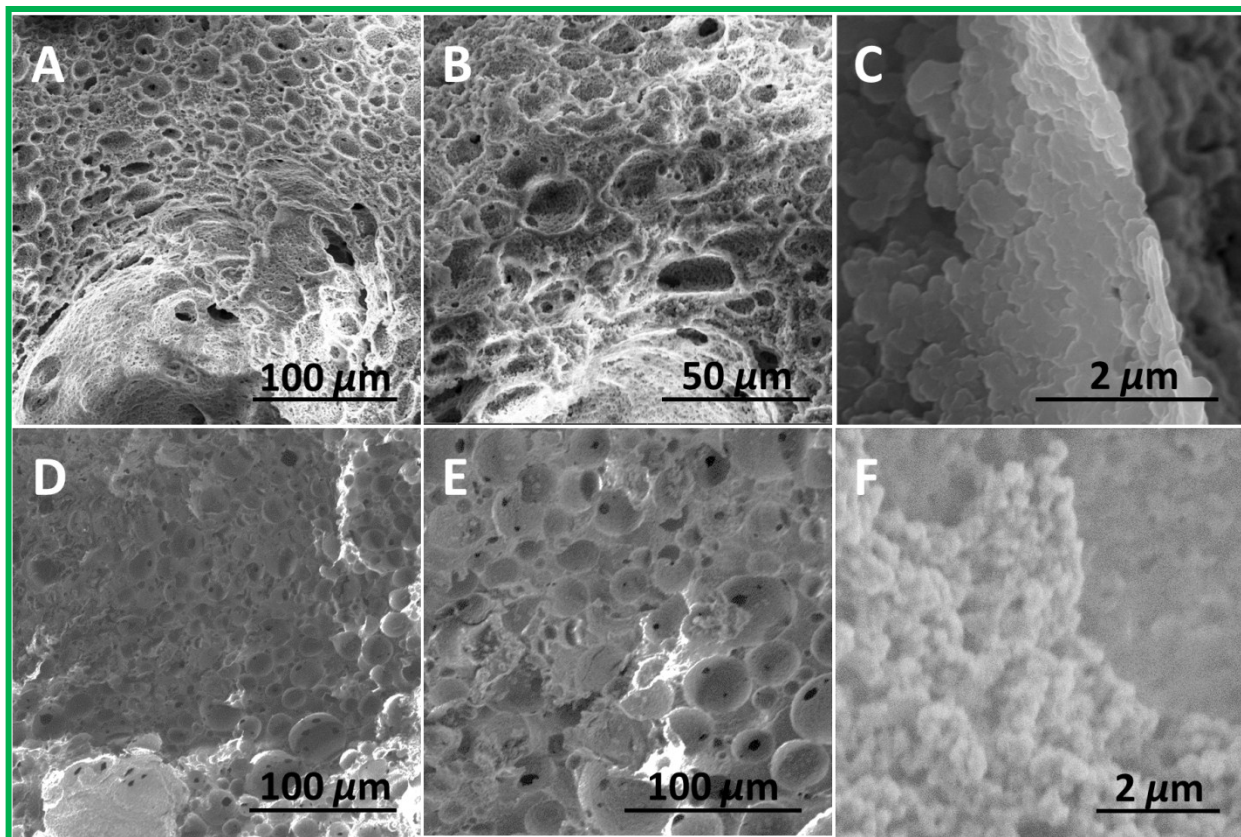
Figure S2. SEM images (cross-sectional view) of (A−C) PAM showing greater macroporosity, (D−F) PAM−TiO$_2$ NC macrobeads showing (D,E) blocked pores and (F) TiO$_2$ particles.
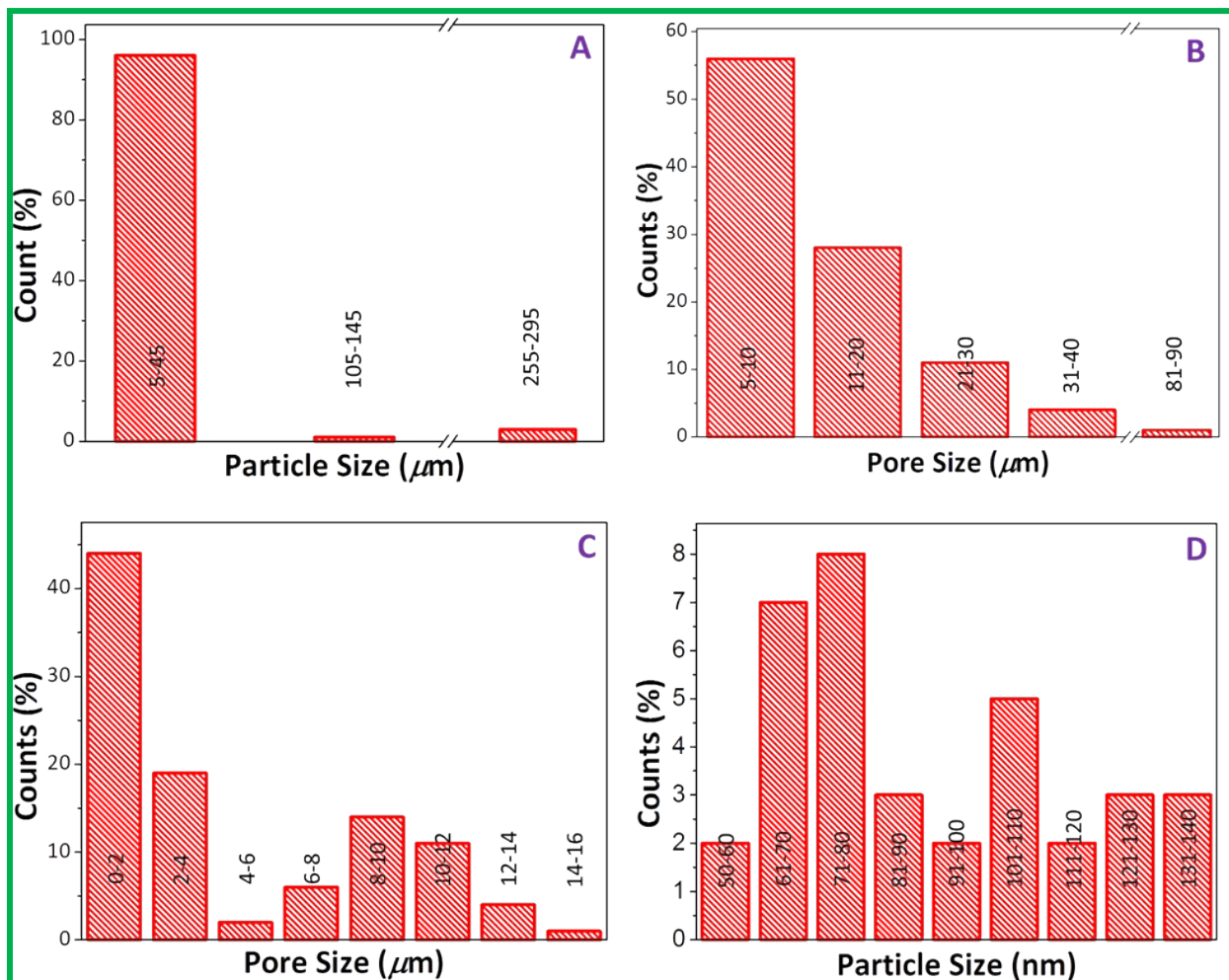
Figure S3. Pore size distribution of (A) PAM, (B) PAM−TiO$_2$ NC and (C) porous NS TiO$_2$ macrobeads. (D) Particle size distribution of TiO$_2$ nanobuilding blocks. ImageJ software was used to measure the average pore size distribution of beads and particle size of TiO$_2$ nanobuilding units (NBUs).
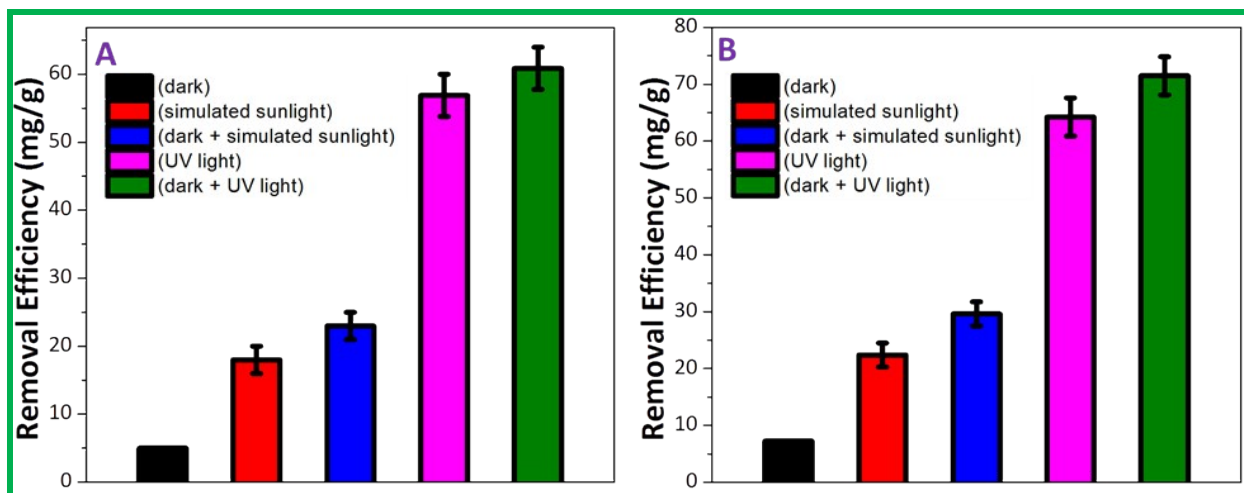
Figure S4. Removal efficiency (mg/g) of porous NS TiO_2 macrobeads (A) without H_2O_2, and (B) with H_2O_2.
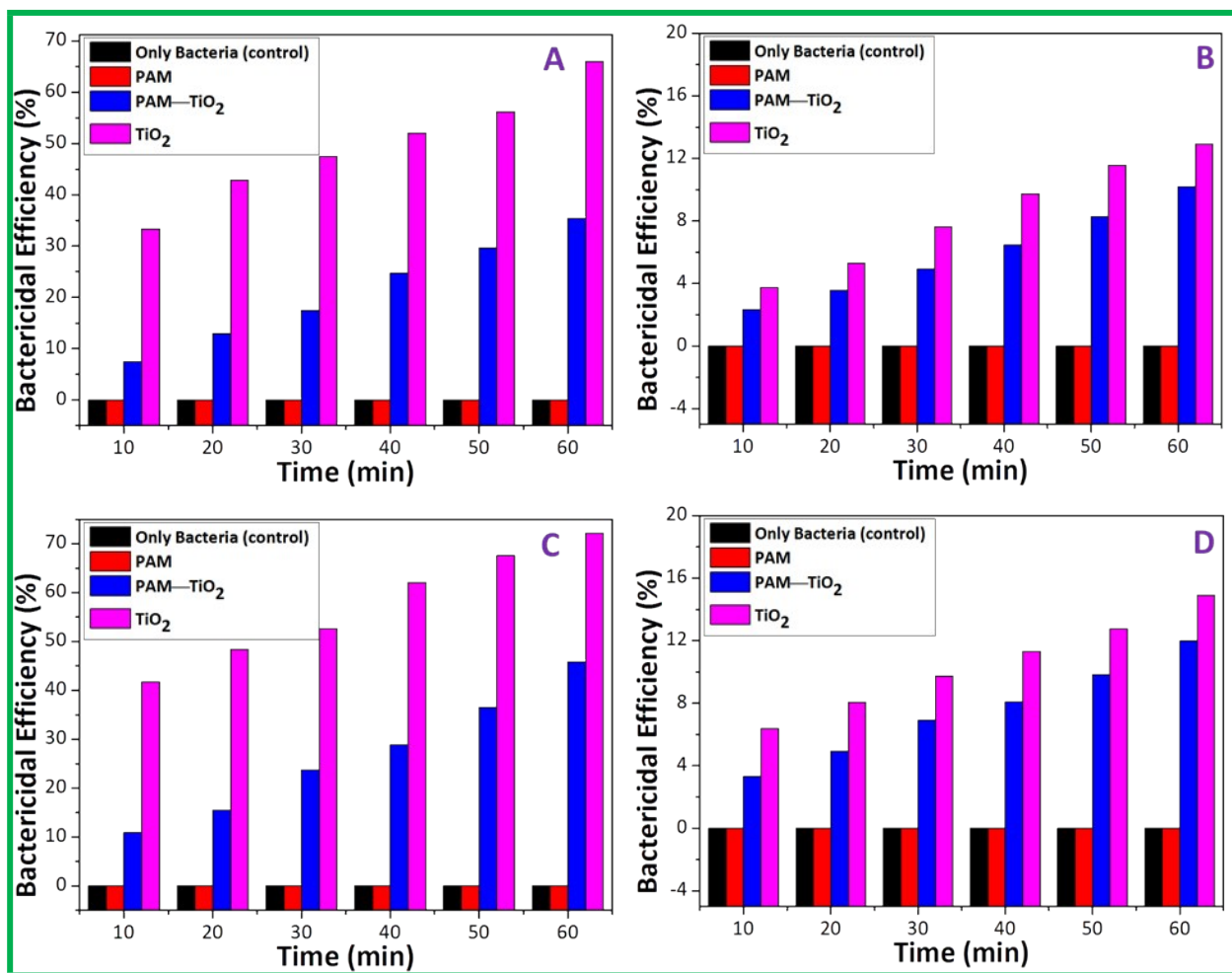
Figure S5. Time-wise bactericidal efficiencies (%) of 0.2 mg/mL dosage of PAM, PAM−TiO_2 NC and porous NS TiO_2 macrobeads against *S. aureus* under (A) UV light and in the (B) dark, and against *E. coli* under (C) UV light and in the (D) dark.
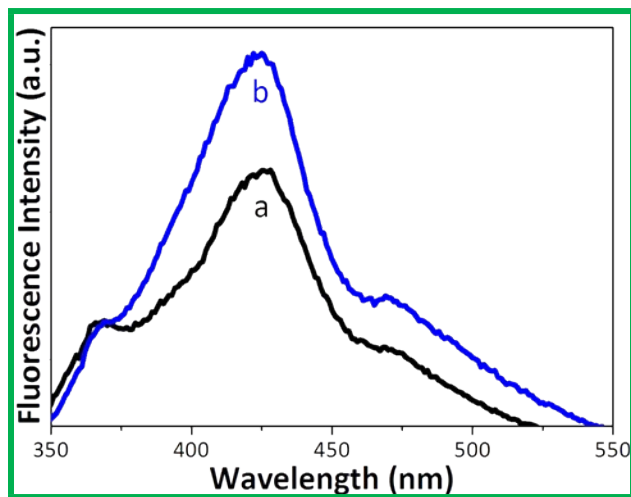
Figure S6. Fluorescence spectra of the irradiated (a) TA (without TiO_2) and TA with TiO_2 samples.
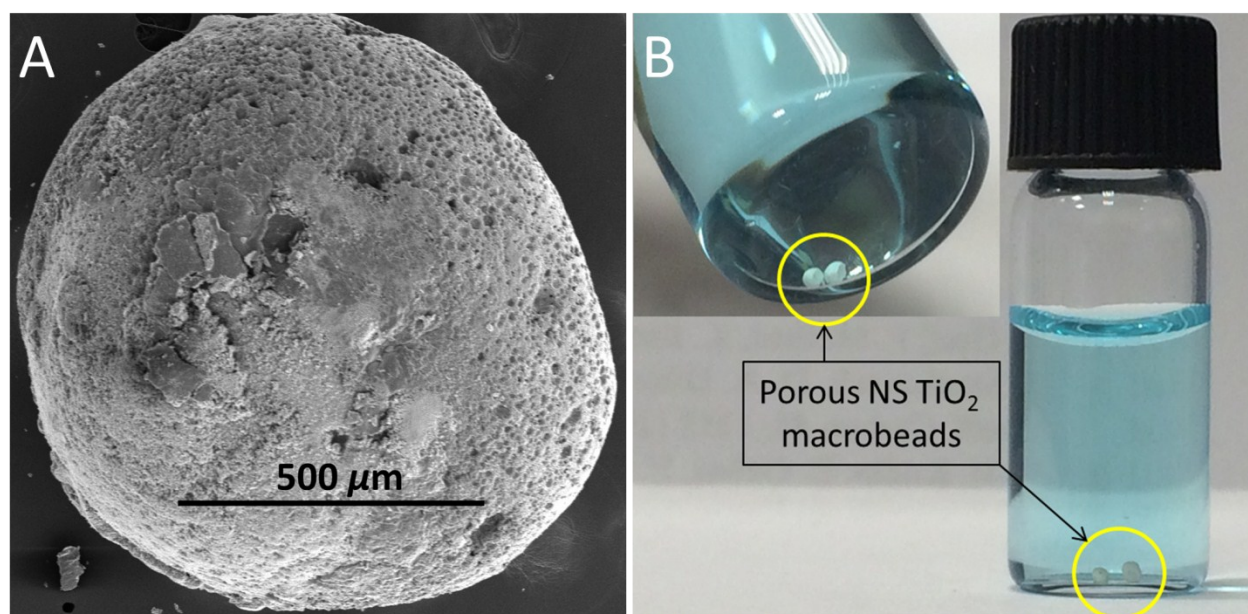
Figure S7. SEM image of a single NS TiO$_2$ macrobead. (B) Digital photograph of the NS TiO$_2$ macrobeads (zoomed-in view in the inset) showing their integrity in MB aqueous solution.

Table S1. A comparison for the removal of methylene blue by different TiO_2-based materials.

Material	Removal Efficiency	k (min⁻¹)	Operational Parameters				Ref.
			mg of Catalyst	MB Conc.	mL of MB	min	
commercial TiO_2 powders	48.2%	—	15	20 ppm	50	70	1
CdSe-TiO_2 nanocrystals	67%	0.004	9	10 ppm	100	60	2
TiO_2–polymer nanofibers	70%	—	—	1×10^{-5} M	200	180	3
TiO_2-based coatings	71.5%	—	10	2×10^{-5} M	10	180	4
Ag NPs loaded TiO_2 NTs	81.2%	—	20	20 ppm	60	150	5
PoPD/TiO_2 NCs	85.9%	0.010	30	10 ppm	30	180	6
commercial TiO_2 NPs	90%	0.025	150	150 ppm	300	360	7
anatase nano-TiO_2	90.3%	0.035	50	4×10^{-5} M	100	60	8
TiO_2 hollow microspheres	92%	—	100	15 ppm	500	360	9
TiO_2@rGO NCs	92%	0.018	200	—	5	120	10
Ag@Fe$_3$O$_4$@SiO$_2$@TiO$_2$	95% 51 mg/g	—	10	50 ppm	20	240	11
JHP-TiO_2-Au microswimmer	97%	—	1	10^{-6} M	—	60	12
chargeable TiO_2 NPs	97%	0.018	100	10 ppm	600	180	13
electrospun fiber embedding TiO_2 [(EPF(2/1)–TiO_2]	97% (total)	0.045 0.050	—	20 μM 10 μM	—	330	14
porous TiO_2 nanowires	97.98%	—	15	20 ppm	50	56	15
aerochitin-TiO_2 composite	98%	0.018	10	10 ppm	10	200	16
NS TiO_2 macrobeads (without H_2O_2)	86.87% (total) 60.89 mg/g	0.030	5 3	25 ppm	10	60	This study
NS TiO_2 macrobeads (with H_2O_2)	98.53% (total) 64.24 mg/g	0.050	5 3	25 ppm	10	60	

Total means the cumulative efficiency achieved under both the dark and UV light conditions; K is the reaction rate constant; MB stands for methylene blue; conc. stands for concentration; ref. stands for references; NTs, NPs, NCs and NS stand for nanotubes, nanoparticles, nanocomposites and nanostructured, respectively.

References

1. J. Huang, H. Ren, X. Liu, X. Li and J.-J. Shim, *Superlattices Microstruct.*, 2015, **81**, 16-25.

2. I. A. Mir, I. Singh, B. Birajdar and K. Rawat, *Water Conserv. Sci. Eng.*, 2017, **2**, 43-50.

3. A. Abdal-hay, A. S. Hamdy Makhlouf and K. A. Khalil, *ACS Appl. Mater. Interfaces*, 2015, **7**, 13329-13341.

4. F. Xu, T. Wang, H. Chen, J. Bohling, A. M. Maurice, L. Wu and S. Zhou, *Prog. Org. Coat.*, 2017, **113**, 15-24.

5. P. Van Viet, B. T. Phan, D. Mott, S. Maenosono, T. T. Sang and C. M. Thi, *J. Photochem. Photobiol., A.*, 2018, **352**, 106-112.

6. C. Yang, M. Zhang, W. Dong, G. Cui, Z. Ren and W. Wang, *PloS one*, 2017, **12**, e0174104.

7. M. Subramaniam, P. Goh, N. Abdullah, W. Lau, B. Ng and A. Ismail, *J. Nanopart. Res.*, 2017, **19**, 220.

8. J. Zhang, B. Wu, L. Huang, P. Liu, X. Wang, Z. Lu, G. Xu, E. Zhang, H. Wang and Z. Kong, *J. Alloy. Compd.*, 2016, **661**, 441-447.

9. J. H. Pan, X. Zhang, A. J. Du, D. D. Sun and J. O. Leckie, *J. Am. Chem. Soc.*, 2008, **130**, 11256-11257.

10. M. Sohail, H. Xue, Q. Jiao, H. Li, K. Khan, S. Wang and Y. Zhao, *Mater. Res. Bull.*, 2017, **90**, 125-130.

11. J. Su, Y. Zhang, S. Xu, S. Wang, H. Ding, S. Pan, G. Wang, G. Li and H. Zhao, *Nanoscale*, 2014, **6**, 5181-5192.

12. V. Sridhar, B. W. Park and M. Sitti, *Adv. Funct. Mater.*, 2018, **28**, 1704902.

13. F. Azeez, E. Al-Hetlani, M. Arafa, Y. Abdelmonem, A. A. Nazeer, M. O. Amin and M. Madkour, *Sci Rep.*, 2018, **8**, 7104.

14. C.-G. Lee, H. Javed, D. Zhang, J.-H. Kim, P. Westerhoff, Q. Li and P. J. Alvarez, *Environ. Sci. Technol.*, 2018, **52**, 4285-4293.

15. Y. Tang, H. Ren and J. Huang, *Front. Optoelectron.*, 2017, **10**, 395-401.

16. R. S. Dassanayake, E. Rajakaruna and N. Abidi, *J. Appl. Polym. Sci.*, 2018, **135**, 45908.